Macroporous glass-ceramic materials with bioactive properties

C. VITALE-BROVARONE*, S. DI NUNZIO, O. BRETCANU, E. VERNÉ
Materials Science and Chemical Engineering Department, Polytechnic of Torino, C.so Duca degli Abruzzi 24, 10129 Torino, Italy
E-mail: chiara.vitale@polito.it

In the present research work, glass powders and three different organic starches were used to realize macroporous glass-ceramic scaffolds for bone substitutions.

For this purpose, bioactive glass powders belonging to the system SiO_2–CaO–Na_2O–MgO were mixed in a liquid medium with the desired amount of the selected organic phase. Afterwards, by progressively raising the temperature, the water uptake of starches occurred and led to the gelling of the whole system. The resultant gel underwent two thermal treatments in order to eliminate the organic phase and to allow the sintering of the glassy phase. In this way, macroporous glass-ceramic scaffolds were successfully prepared. The samples were characterized by means of optical and scanning electron microscopy with compositional analysis. The volume and mean size of the obtained porosity were investigated by means of mercury intrusion porosimetry, whereas its morphology was assessed by means of microscopic observations. The structure of the original and the resultant materials were investigated by X-ray diffraction. In order to study the reactivity of the scaffolds towards physiological media, the samples were soaked in a simulated body fluid for various times. On their soaked surfaces, scanning electron microscopy and compositional analysis were carried out in order to assess their bioactivity.

Introduction

Autogenous and allogenic bones have been considered, for a long time, the best solutions for bone substitutions. In fact, both of them provide a satisfactory and fast osteointegration with the surrounding tissues. Despite this, some concerns on their use still remain [1–3]. For the autogenous bone, these concerns are the following ones:

- the donor site morbidity (which is a direct consequence of the explant);
- a limited availability.

As far as the allogenic bones are concerned, there are still many worries about the possible risks of disease transmission and also some psychological reservation from the receiving patients.

For the above mentioned reasons, many synthetic biomaterials have been studied as bone substitutes in the orthopaedic and maxillofacial surgery. Among them, the ceramic materials have been increasingly investigated in the recent years by many researchers [4–8].

A satisfactory bone substitute should be biocompatible and preferentially osteoinductive in order to stimulate the growth of healthy bone on its surface.

Among ceramic materials, some glasses and glass-ceramics show bioactive properties. In fact, these biomaterials are able, by a complex mechanism of interaction with the surrounding biological fluids, to induce the precipitation of a hydroxylapatite (HAp) layer on their surfaces. This biologically active layer of HAp will be considered as itself by the surrounding living tissues and for this reason, its presence is widely accepted as proof of the ability of these materials to bond with hard tissues [9–11]. Some of these bioceramics are already used in different forms, such as granule, bulk or coating materials in a certain number of applications where a chemical bond with the surrounding bone is required [12–17]. In addition, most of the glasses with high contents of alkaline oxides can undergo a severe or complete dissolution when in contact with physiological fluids [9] and for this reason they can also be considered as good candidates for bioresorbable implants.

Besides being bioactive, a proper bone substitute should also be able to guide the bone regeneration into the defect. For this reason it has to be in a macroporous form in order to provide a correct blood supply inside the implant as well as a satisfactory bone in-growth.

Therefore, the synthetic ceramic scaffold should have a high volume of macropores in the range of 50–150 μm, highly interconnected.

*Author to whom correspondence should be addressed.

To realize macroporous materials fulfilling the above mentioned requirements, different methods have been proposed such as: soaking of cellulose sponges, gravity sintering method, foaming of a ceramic suspension with H_2O_2, solid freeform fabrication and starch consolidation [18–26]. For its simplicity and versatility, among the latter methods, we decided to use the starch consolidation, already applied with success to other materials [23–25].

This method employs starch powders as consolidation agents of a suspension due to their ability of absorbing water when heated. After the water uptake has occurred, the organic phase is completely driven off by means of a thermal treatment and thus it acts as a pore forming agent. Once the burning out of the starches has been completed, the inorganic phase is sintered.

Up to now, this method has been used whether with ceramic materials such as alumina (not for biomedical applications) [23] or calcium carbonate [24] or with mixtures of HAp and a phosphate glass [25].

For these materials, the HAp formation on the materials surface after soaking in simulated body fluid (SBF) was not assessed as only other calcium phosphates were found [24]. Besides, in the recent literature, only glasses containing P_2O_5 were used to prepare macroporous scaffolds and for most of them P_2O_5 was the glass former (invert glasses).

On the basis of the above mentioned considerations, it was decided to consider the application of this technique to the preparation of P_2O_5-free glass-ceramic scaffolds with bioactive properties. The P_2O_5-free glass composition was chosen on the basis of our previous results [13, 15], where a $SiO_2-CaO-Na_2O$ base-glass (named SCN) was used to produce bioactive composites and coatings. In this work, it was also shown that, by a proper thermal treatment of this glass, a final glass-ceramic structure containing $Na_2Ca_2(SiO_3)_3$ crystals could be obtained. This glass-ceramic showed a good sintering ability and also an elevated degree of bioactivity. The high bioactivity index of $Na_2Ca_2(SiO_3)_3$ was also confirmed by other authors [27].

Many authors have stressed the positive effect of Mg^{2+} on many cellular functions [28–29] and have also proved its positive outcome on the formation of the HAp layer *in vitro* [30].

For the above mentioned reasons, in this work, a certain amount of MgO was added to the base glass SCN and a new glass, that will be subsequently named SNCM, was prepared. The choice of a proper glass composition and of an optimized sintering treatment led to a final glass-ceramic system with $Na_2Ca_2(SiO_3)_3$ as crystalline phase. A glass-ceramic structure might present several advantages versus both glassy and fully crystalline ones. In fact, by means of proper modifications of the amount of the crystalline versus the amorphous phase and by selecting the proper glass composition, it should be possible to obtain, if needed, a partially resorbable system with a proper resorbing kinetic.

As far as the organic phase is concerned, different types of starches were used (corn, potatoes and rice) and three different relative amounts. The starch content and also the solid loading were modified in order to optimize the process and to reach a good compromise in terms of the amount of porosity and a sufficient consistence of the sintered scaffold.

Materials and methods

In this research work, both organic and inorganic materials were used to prepare macroporous glass-ceramic scaffolds through the burning-out of the organic phase and the sintering of the inorganic one.

As far as the organic phase is concerned, three commercial organic additives (corn, potatoes and rice starches) were used as both pore formers and consolidation agents. The starch powders were sieved above 63 μm in order to select the larger particles. Instead, the inorganic phase consisted of a bioactive glass, named SNCM, belonging to the $SiO_2-Na_2O-CaO-MgO$ system. In this quaternary system, the glass composition was tailored in order to crystallize $Na_2Ca_2(SiO_3)_3$ and to contain a sufficient amount of MgO. The final glass composition was set as follows: 50 SiO_2, 25 Na_2O, 16 CaO, 9 MgO (molar %).

SNCM was prepared by melting the starting products (SiO_2, Na_2CO_3, $CaCO_3$ and $MgCO_3$) in a platinum crucible at 1500 °C for 1 h and by quenching the melt in cold water. Afterwards, the quenched SNCM was grounded and sieved to a final grain size below 106 μm.

Bulk preparation

Weighed amounts of one starch and of SNCM were mixed with a proper amount of distilled water in order to obtain a slip with a certain solid loading. The suspension was magnetically stirred in order to obtain a homogenous dispersion of the powders. After 1 h of stirring, the slip was slowly heated until 70–80 °C while maintaining the magnetic agitation.

At temperatures ranging from 70–80 °C and depending on the type of starch, a remarkable water uptake occurred. In such a way, the swelling of the organic phase led to the gelling of the whole suspension; a conspicuous increase of the system viscosity was observed as any further movement of the magnetic stirrer was hindered. After gelling, the system was promptly poured in a metallic mould and underwent a consolidation treatment at about 80 °C in order to remove the residual water. Once the consolidation step was over, the samples underwent a sequence of two different thermal treatments. Specifically, these treatments consist of a burnout step (necessary to drive off the organic phase) and of a subsequent sintering phase to densify the inorganic phase (SNCM).

The above described treatments led to the preparation of a macroporous scaffold.

Three different series of samples were prepared in order to ascertain the influence of the processing parameters (amount of organic phase, thermal treatment and solid loading), on the final structure of these macroporous scaffolds.

Table I reports the chosen experimental parameters for each series of samples as well as their acronyms (the letter indicates the type of starch: corn, potatoes and rice and the number, the content of the organic phase (wt %).

TABLE I Experimental parameters for the three series of samples

Sample	Organic phase (% wt)	Solid loading (%)	Sintering T [°C]
C14	14	20	900
P14	14	20	900
R14	14	20	900
C20	20	25	900
P20	20	25	900
R20	20	25	900
C26	26	40	900
P26	26	40	900
R26	26	40	900

Materials characterization

In order to assess the size and shape of the starting materials, on both the organic starches and the SNCM powders, a morphological evaluation by means of scanning electron microscopy (SEM Philips 525M) was carried out.

The structure of the as done SNCM powders, that should be completely amorphous, was investigated by X-ray diffraction (X'Pert Philips diffractometer) using the Bragg Brentano camera geometry and the CuK_{α} incident radiation. In addition, on SNCM powders, a differential thermal analysis was carried out to evaluate its characteristic temperatures (DTA Netzsch 404 S).

All the prepared scaffolds were observed by SEM equipped with compositional analysis (energy dispersive spectrometer: EDS, Philips-EDAX 9100). In this way, the degree of sintering achieved during the thermal treatment as well as the size, morphology and distribution of the introduced macroporosity were assessed. EDS analyses were also carried out in order to verify that the composition of the starting powders and of the prepared scaffold were consistent with the SNCM theoretical one.

The aim was to acquire a quantitative evaluation of the amount and size of the obtained macroporosity, on the most representative samples, mercury intrusion porosimetry studies (FISONS macropores unit 120) were performed.

X-ray analyses were carried out on the scaffolds in order to verify if the thermal treatment induced any crystallization phenomena on the starting amorphous SNCM leading to a final glass-ceramic material. Also if an influence of the starches on the SNCM crystallization was unlikely, nevertheless, to support this forecast, the proposed sintering treatment was carried out on pure SNCM powders.

From the biological point of view, the *in vitro* behaviour of the realized biomaterials was investigated by soaking them in a simulated body fluid, which has almost the same ion concentrations of the human plasma [31].

At this point, samples with about 1 cm^2 area were soaked in 25 ml of SBF in polyethylene bottles and maintained at 37 °C for periods up to 4 weeks, without stirring or refreshing the solution. After soaking, the scaffolds were characterized by means of SEM with EDS in order to evaluate the presence, morphology and thickness of the hydroxylapatite layer precipitated on their surfaces.

Results

The three organic phases, when observed at SEM showed a globular morphology, particularly the potatoes and rice starches. Moreover, as observed in Fig. 1(a), (b) and (c), they all show a certain tendency to agglomeration. Among them, the corn starch showed the smallest particles. As observable in Fig. 1(c), the rice starch

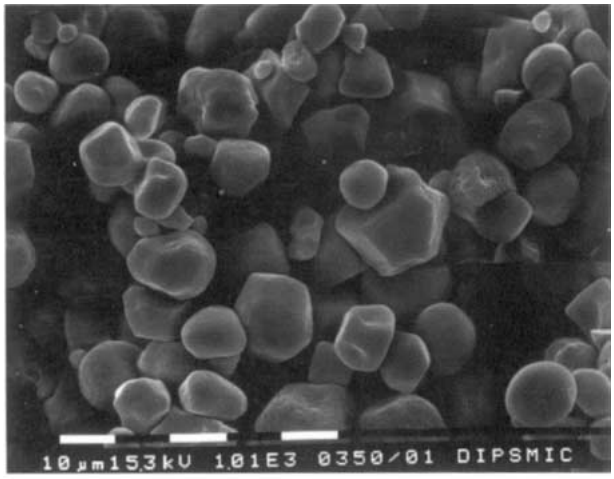

(a)

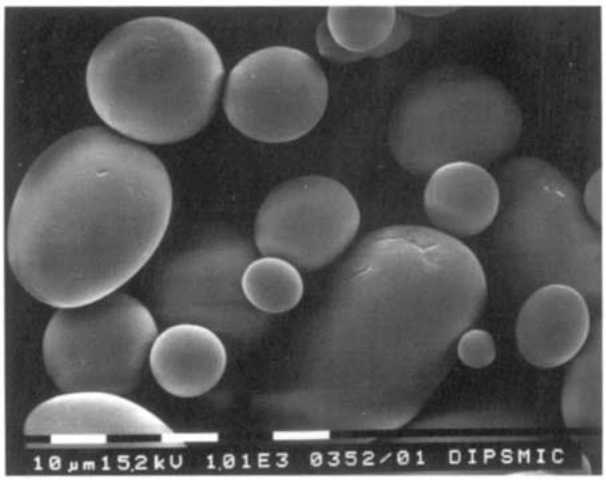

(b)

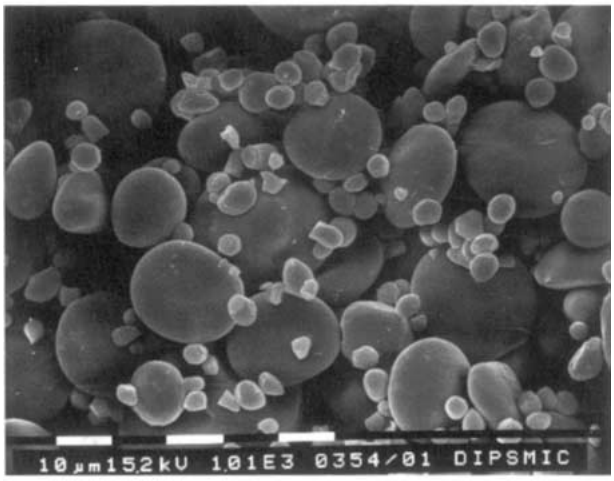

(c)

Figure 1 Corn (a), potatoes (b) and rice (c) starches micrographs.

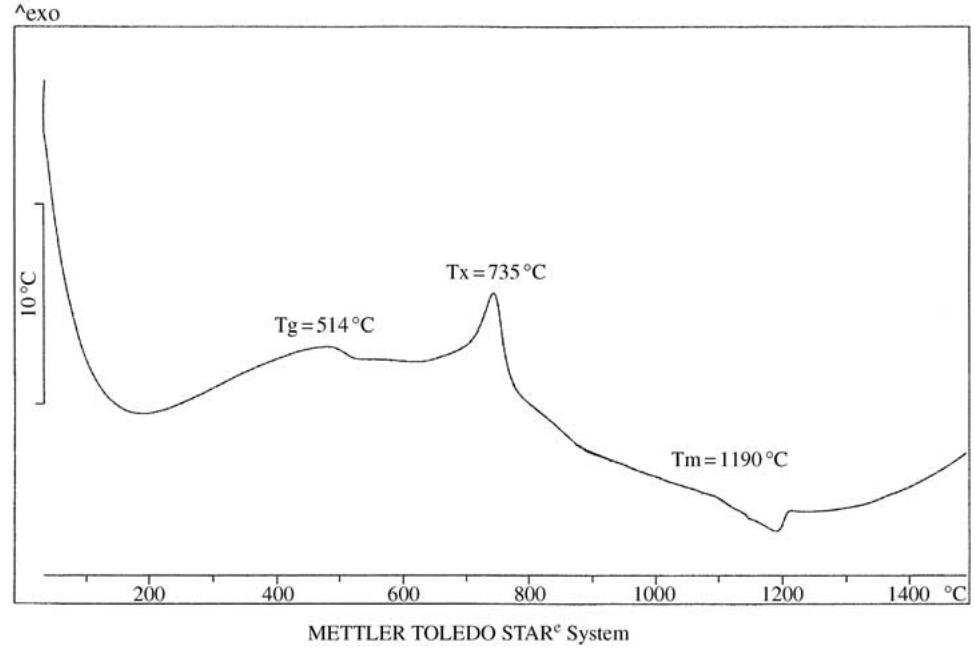

Figure 2 Differential thermal analysis of as done SNCM.

presents a bimodal distribution of the particle sizes and for this reason, the sieving phase was particularly important for it in order to avoid the presence of too small particles.

SNCM was thermally characterized and the results of its DTA analysis are reported in Fig. 2. The DTA curve shows a glass transition temperature at 514 °C, a crystallization peak around 735 °C and an endothermic peak between 1100 and 1190 °C (liquidus/melting temperature).

The structure of SNCM was investigated by X-ray diffraction and the resulting pattern is reported in Fig. 3. The as done SNCM (pattern a) shows only an amorphous halo within 25 and 37 °C and this confirms that the starting SNCM powders were completely amorphous. In Fig. 3 are also reported the patterns of sintered SNCM (b) and of P14 macroporous sample (c) and it can be noticed that they differ completely with respect to as done SNCM. In fact, the superimposition of these patterns highlights that for the sintered materials, the amorphous halo has almost completely disappeared whereas many diffraction peaks can now be seen. These peaks are identical for P14 and for sintered SNCM and this confirmed that the presence of the starch did not influence at all the crystallization phenomenon. Besides, the most intense diffraction peaks are in correspondence with the amorphous halo of SNCM, as usually happens when a glass is crystallized. All the diffraction peaks were identified with the above mentioned sodium-calcium silicate $Na_2Ca_2(SiO_3)_3$.

The samples of the first series (C14, P14 and R14) were prepared by mixing 14 wt % of the corresponding starch with SNCM powders in a liquid medium with a solid loading of 20%.

The slip was vigorously stirred for 1 h and then heated till 75–80 °C when a remarkable and sudden water uptake took place, leading to a noticeable and instantaneous viscosity increase of the slip. In this way, the liquid suspension turned into a gel like material that was poured

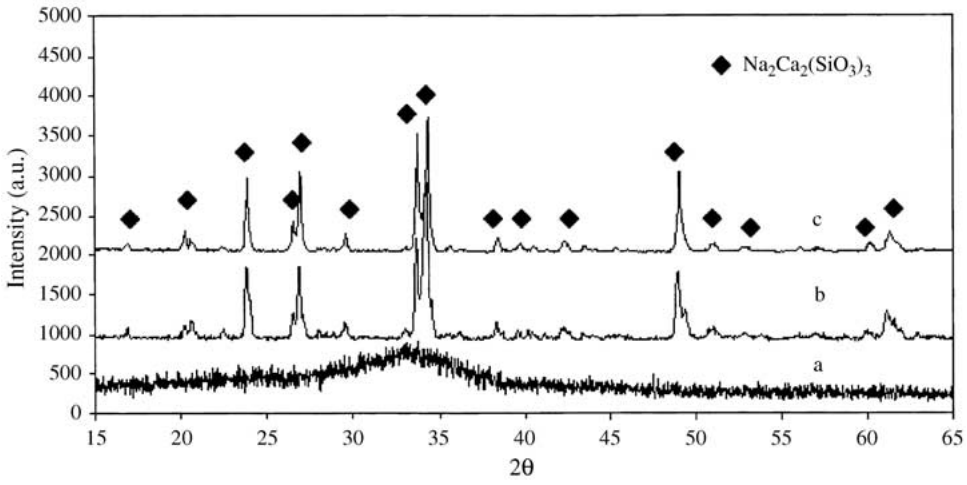

Figure 3 X-ray diffraction patterns of as done SNCM (a), sintered SNCM (b) and P14 (c).

in a metallic mould. The influence of the slip viscosity on the gelling properties of the starch was not investigated (it was outside our study) and literature data were taken into account in order to optimize this step [23]. Afterwards, a consolidation treatment was carried out on the samples by heating them at 80 °C for 12 h and then for 2 h at 130 °C. During this treatment, the samples underwent a remarkable shrinkage and the formation of some transversal cracks occurred. After consolidation, the samples were de-molded and a burnout treatment was carried out in order to allow the formation of decomposition products and their gradual removal. This latter treatment was set as follows:

- heating the sample at 300 °C for 1 h;
- increasing the temperature (rate 1.5 °C/min) till 700 °C;
- cooling till room temperature (rate 5 °C/min).

After this step, only the inorganic phase is left and needs to be sintered to impart sufficient mechanical strength to the samples. At this purpose, the samples were heated till 900 °C (rate 5 °C/min) and maintained at this temperature for 3 h.

Fig. 4(a)–(c) show the morphology of the first series of samples. In these micrographs, rough surfaces and the presence of crystals can be observed and are a proof of the glass-ceramic nature of these materials. The good sintering level of these biomaterials is assessed by the presence of numerous intergranular necks. Interconnected macroporosity with average size of about 10–30 μm can be observed for samples P14 and R14, while sample C14 seems to be denser.

The samples of the second series were prepared by increasing the starch content till 20 wt % (C20, P20 and R20) in order to increase the amount of introduced porosity. Also the solid loading was raised up to 25% in order to reduce as much as possible the uneven shrinkage that was observed for series 1 samples.

As far as the consolidation step is concerned, the maintenance at 130 °C was omitted as it caused problems of material sticking to the metallic mould without offering any observable benefits.

As far as the burnout and the sintering treatments are concerned, they were kept identical to those used for series 1 samples.

On the prepared scaffolds, after the consolidation treatment was over, an uneven shrinkage was observed and due to it, some transversal cracks formed. These cracks were not sealed during the subsequent sintering stage.

Fig. 5(a)–(c) report some micrographs of series 2 samples: also for these samples, a high sintering level was obtained. Besides, in these micrographs, interconnected macroporosities with average sizes of 20–40 μm are found for samples C20 and P20 and of about 80–100 μm for R20.

For the third series of samples (C26, P26 and R26), as the problems related to the uneven shrinkage of the consolidated green were still present, the solid loading was further increased to 40% and the consolidation treatment was modified.

In order to allow a more gradual consolidation of the poured gel, the following schedule was developed: maintenance for 30 min at 40–60 °C, for 2 h at 65 °C and 75 °C and for 12 h at 80 °C. Moreover, in order to promote both a sufficiently slow decomposition of the organic additives and a better sintering of the inorganic phase, the burnout and the sintering phases were combined. In fact, the proposed thermal treatment for the third series of samples, consisted of a slow heating (1 °C/min) till 900 °C with a maintenance at 300 °C for 1 h and another one at 900 °C for 3 h.

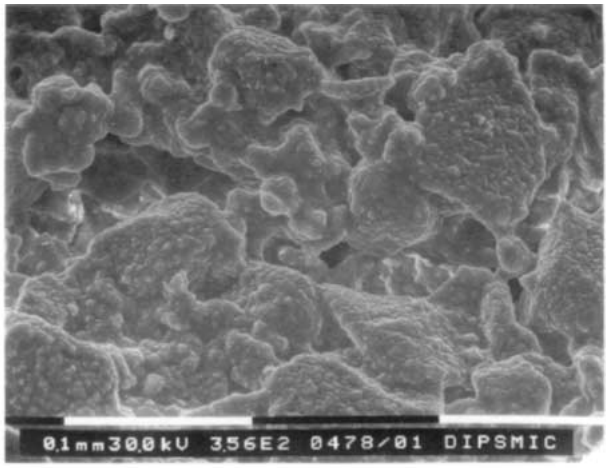

(a)

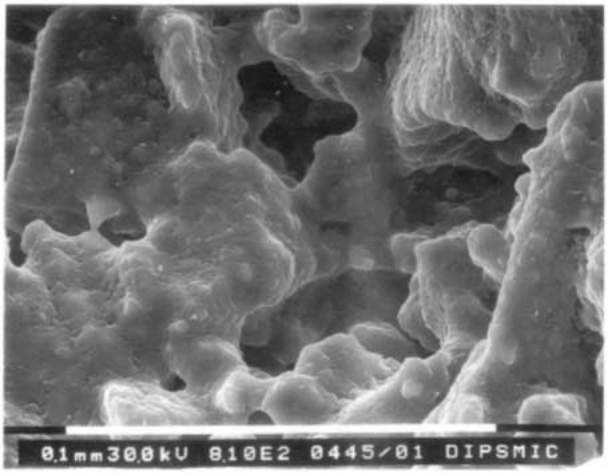

(b)

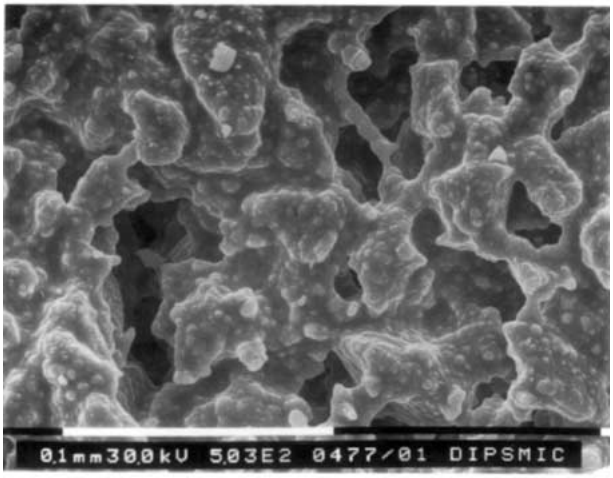

(c)

Figure 4 Micrographs of samples C14 (a), P14 (b) and R14 (c).

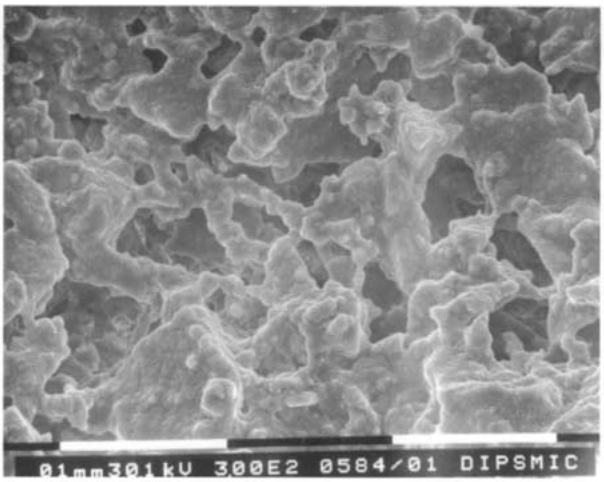

(a)

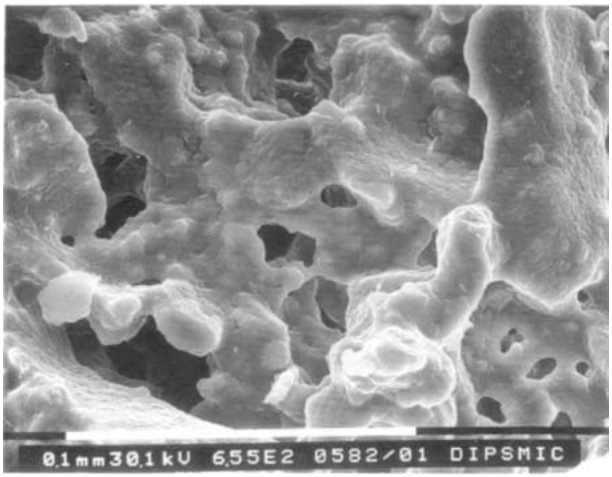

(b)

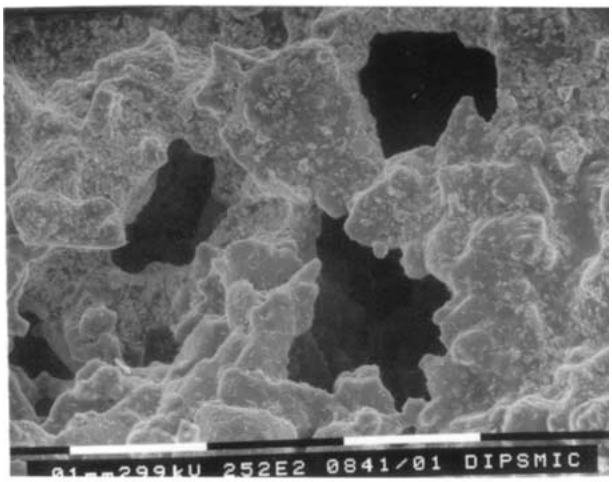

(c)

Figure 5 Micrographs of samples C20 (a), P20 (b) and R20 (c).

As far as the resulting microstructure is concerned, Fig. 6(a), (b) report two micrographs of sample P26 at different magnifications.

As can be observed in Fig. 6(a), the distribution of the porosity is quite homogeneous and its amount is definitely higher than the one observed for series 1 and 2. Moreover, as demonstrated by Fig. 6(b), the macroporous sizes are for this series, about 100–500 μm. Unfortunately, the degree of sintering of these samples is not completely satisfactory as the pore walls are not dense enough.

Fig. 7 reports the results of a number of mercury intrusion porosimetry analyses carried out on some representative samples of the three series.

The *in vitro* behaviour of the prepared biomaterials was investigated by soaking them in SBF for periods up to 4 weeks. The obtained results were analogous for all the samples and were highly satisfactory.

In fact, after 4 weeks of soaking, all the samples showed an extensive precipitation of hydroxylapatite on their surfaces and also inside the macropores.

Fig. 8(a), (b) report two micrographs of samples P14 and R20 after 4 weeks in SBF. The presence of many globular agglomerates of hydroxylapatite distributed all over the surface and inside the macropores can be observed.

Fig. (9) shows the results of a compositional analysis performed on the whole area reported in Fig. 8(a). The

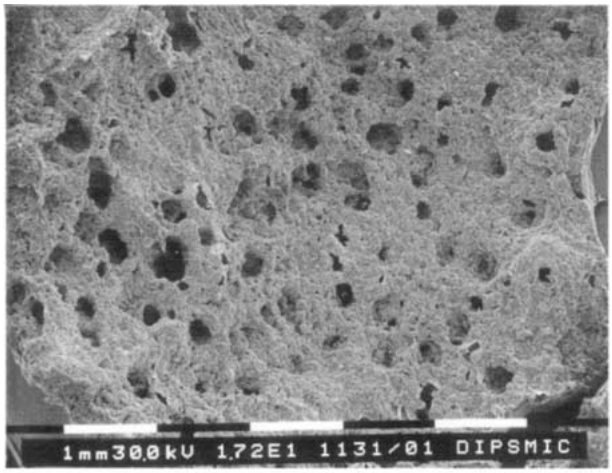

(a)

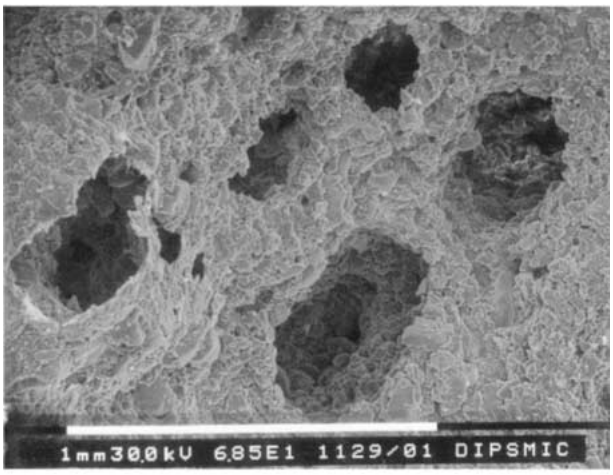

(b)

Figure 6 Micrographs of sample P26; (a) general view, (b) detail of macropores.

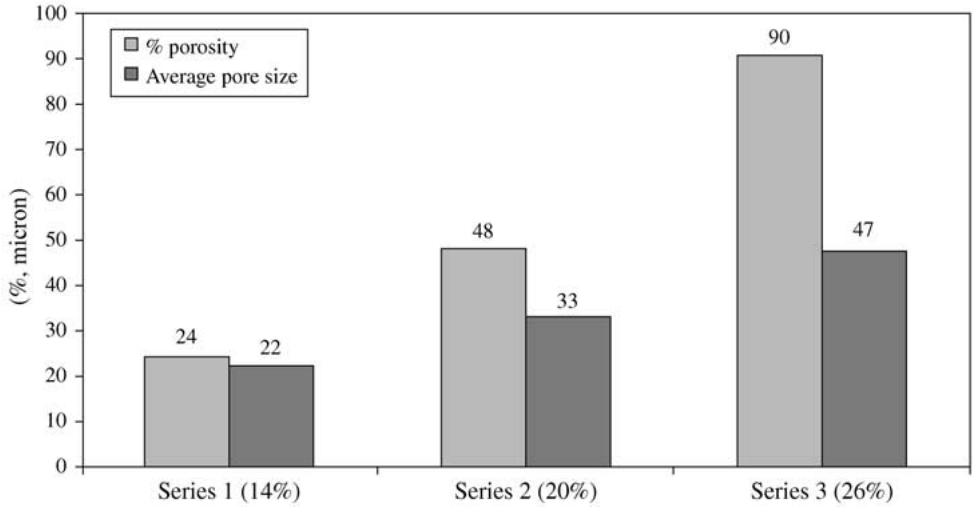

Figure 7 Mercury intrusion porosimetry results for the three series of samples.

average EDS analysis on this area revealed only the presence of Si, Ca and P ions, with a Ca/P weight ratio close to 2.15 (i.e. the theoretical value for hydroxylapatite) (Fig. 9).

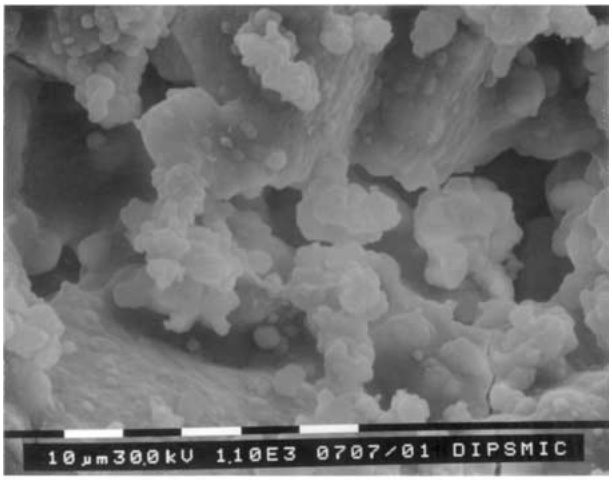

(a)

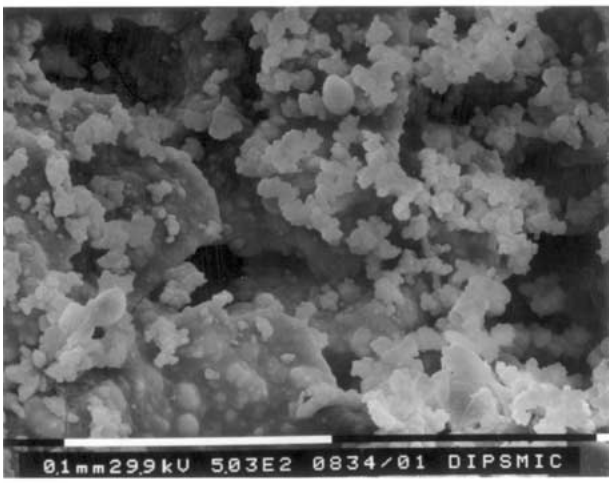

(b)

Figure 8 Micrographs of samples P14 (a) and R20 (b) after 4 weeks in SBF.

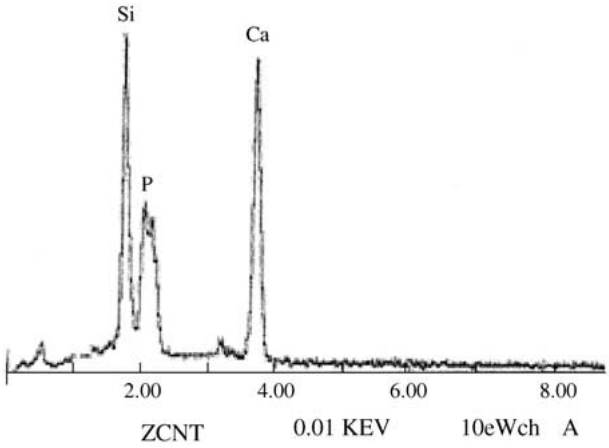

Figure 9 EDS results of the analysis carried out on the whole area reported in Fig. 8(a) (P14 after 4 weeks in SBF).

Discussion and conclusion

The starches micrographs reported in Fig. 1(a)–(c) show that the biggest particles ranged from 20 µm (corn starch) up to 70–80 µm (potatoes and rice starch). For this reason, the powder sizes were selected using a proper sieve (63 µm) in order to attain the largest particle sizes. Nevertheless, as for all the starches a certain tendency to agglomeration was observed, it is only possible to state that the main particles fraction was above 63 µm.

The thermal characterization highlighted the presence of a crystallization peak at 735 °C and of a liquid/melting point just below 1200 °C. On the basis of these findings, the sintering temperature was chosen in order to fulfill two main requirements. In fact, the sintering temperature should be:

- not too close to the liquidus one in order to allow the maintenance of the introduced macroporosity;
- not too low in order to guarantee a sufficient degree of sintering.

The correct choice of the sintering temperature led to a good compromise between a well-sintered and thus mechanically resistant material, and a highly porous structure.

As far as Fig. 3 is concerned, the absence of diffraction

peaks and the presence of an amorphous halo are consistent with the amorphous nature of as done SNCM. On the other hand, as shown by the diffraction patterns of sintered SNCM and of sample P14, many crystallization peaks appeared after sintering. Yet, as the sintering treatment was carried out above the crystallization temperature of SNCM, a final glass-ceramic structure was expected. The diffraction patterns of sintered SNCM and of the macroporous samples are identical and this confirmed the prediction that the presence of an organic phase and its burning-out did not affect in any way the crystallization phenomenon.

All the diffraction peaks were identified with the sodium–calcium silicate $Na_2Ca_2(SiO_3)_3$ that, as shown by the thermal analysis, crystallizes just above 730 °C.

Mg^{2+} ions are all enclosed in the residual amorphous phase that will be for this reason richer in magnesium oxide. As far as the amount of this residual amorphous phase is concerned, the diffraction patterns proved that the crystallization phenomena occurred to a great extent. In fact, after sintering the amorphous halo almost disappeared and a glass-ceramic with an high amount of crystalline phase was obtained. The prevalence of a crystalline phase versus the amorphous one is in good accordance with the chosen sintering temperature that is 170 °C above the SNCM Tx.

This latter conclusion is also supported by the micrographs reported in Figs. 4 and 5 in which the highly crystalline and not smooth glass-ceramic nature of the samples is observable. Generally, glass-ceramics are very interesting biomaterials as they are more adaptable than pure amorphous or crystalline ones. In fact, by proper calibrations of the nature of the crystalline phases and of the composition and amount of the residual amorphous phase, the final properties of these materials can be tailored. Specifically, it is possible to take advantage of this flexibility by preparing biomaterials with higher or lower surface reactivity and thus with different rates of interaction with the surrounding tissues and degrees of bioactivity. For the above reasons, optimized compositions and thermal treatments might allow, in the future, to obtain glass-ceramic biomaterials with a resorption kinetics matching the rate of bone healing.

Samples belonging to series 1 (14 wt % of starch) showed a good level of sintering and a certain degree of porosity. The resultant microstructure established that the chosen temperature was effective in the achievement of a compromise between the two main requirements: attain a sufficient number of sintering necks and maintain a high residual macroporosity.

Despite this, the SEM observations and the porosimetry results showed that the average macropores sizes were in the range of 20–30 μm and that they were about 20% in volume. These latter values are too low for this study and so some optimizations needed to be done.

In order to attain higher macropores sizes and to increase its amount, the starch content was raised by 20 wt %. Moreover, as on the sintered samples some transversal cracks were observed, to limit the uneven shrinkage, the solid loading was increased for series 2.

As expected, the rise in the organic phase amount, led to a higher degree of macroporosity in terms of both average size and volume content.

The SEM observations showed a homogeneous dispersion of open macropores with a good degree of interconnection and pores sizes in the range of 50–80 μm. The mercury intrusion porosimetry results confirmed these morphological observations and assessed an average macropores size of 50 μm and a volume content above 30%.

Unfortunately, an uneven shrinkage occurred also for this series and for this reason, in series 3, the solid loading was increased up to 40% aiming to obtain a more thick slip. In addition, the consolidation treatment was modified in order to realize a slower and more gradual driving off of the absorbed water. Besides, the burnout phase and the sintering treatment were unified in a single step as the previous results did not highlight any benefits in carrying out these two processes separately. On the other hand, a reduction in the number of treatments would also lead to a more simple and effective technique.

The third series of samples showed a strongly reduced uneven shrinkage as well as a decrease of the transversal cracks. These observations are consistent with the idea of having benefits by the solid loading increase. Despite this, series 3 samples did not show a satisfactory degree of sintering. In fact, many sintering necks can be observed but they are not completely densified. On the other hand, in series 3 samples, a higher amount and size of macropores was obtained as can be stated by observing Fig. 6 and by evaluating the data of the mercury intrusion porosimetry. Mean pores sizes of about 90 μm and pores contents above 45% vol were obtained.

On the basis of these results, it is concluded that the 20–26% starch content range should be better investigated to attain the best compromise between good sintering level and high macropores sizes and content. A 40% solid loading showed to be effective in avoiding cracks formations and uneven shrinkage and forth shape maintenance.

The influence of the type of starch was also investigated but it was difficult to definitely assess which one would be more suitable to the final aims as no substantial difference was observed. Anyway, the corn starch led to the worst results due to its smaller size whereas potatoes and rice ones were more effective.

The *in vitro* tests carried out on all the samples established the high degree of bioactivity of these macroporous biomaterials. In fact, a noticeable hydroxylapatite precipitation was observed for all the samples, regardless of the kind and the amount of the organic additives. The micrographs reported in Fig. 8(a), (b) are representative of all the three series of samples.

On the soaked surfaces, the EDS analyses highlighted the presence of a silica rich layer and of a precipitated hydroxylapatite layer on top of it. In fact, only silicon, calcium and phosphorous were found and in relative amount in good accordance with the former statement. Moreover, the SEM observations assessed that the hydroxylapatite also precipitates inside the interconnected macropores and thus the high degree of bone bonding ability of these biomaterials.

The absence of sodium and magnesium on the soaked surfaces is due to their leaching during the interactions with the surrounding tissues. In fact, SEM observations of

the soaked surfaces showed the appearance of micropores where the amorphous phase was bioresorped. This ion-leaching phenomenon is usually involved in the bioactive mechanism. Specifically, the release of Mg^{2+} would positively affect many cellular functions in the implants proximity. The crystalline phase was not involved in this leaching mechanism but the sodium contained in it could not be detected as a thick HAp layer was present on the soaked surfaces. Though not directly involved in the bioactivity mechanism, as assessed by previous works, $Na_2Ca_2(SiO_3)_3$ is a crystalline phase with a high bioactivity index and so its presence is desirable.

In conclusions the proposed method and the processing parameters seem to be suitable to obtain macroporous glass-ceramic scaffolds with interconnected macroporosity. By a further optimization of the most important parameters such as type and amount of starch amount and, eventually, sintering temperature and time, it would be possible to obtain higher macropores amounts and sizes. The proposed glass composition and the deriving glass-ceramic structure showed a good sintering ability. Besides, a very high degree of bioactivity was observed, even for short soaking periods. For this reason, on the proposed scaffolds a prompt bone in-growth is likely. Biological tests would be proposed in the future to assess the positive effect of Mg^{2+} ions on the cells activity.

As a general conclusion, we believe that glass ceramic bioactive materials are of great scientific interest as their interaction with biological fluids can be modulated to match it with the tissue healing kinetics, giving a valid alternative to conventional ceramic scaffolds.

Acknowledgment

This work was partially granted by ''Giovani Ricercatori 2001 Politecnico di Torino''.

References

1. J. O. HOLLINGER, J. BREKKE, E. GRUSKIN and D. LEE, *Clin. Orthop.* **324** (1996) 55.
2. A. IGNATIUS, C. SCHMIDT, D. KASPAR and L. E. CLAES, *J. Biomed. Mater. Res.* **55** (2001) 285.
3. C. J. DAMIEN and J. R. PARSONS, *ibid.* **2** (1999) 187.
4. W. SUCHANEK and M. YOSHIMURA, *J. Mater. Res.* **13** (1998) 94.
5. T. KOSHINO, T. MURASE, T. TAKAGI and T. SAITO, *Biomaterials* **22** (2001) 1579.
6. K. D. JOHNSONS, K. E. FREIRSON and T. S. KELLER, *J. Othop. Res.* **14** (1996) 351.
7. Y. S. CHANG, M. OKA, T. NAKAMURA and H. O. GU, *J. Biomed. Mater. Res.* **30** (1996) 117.
8. A. OKAZAKI, T. KOSHINO, T. SAITO and T. TAKAGI, *Biomaterials* **21** (2000) 483.
9. H. KIM, F. MIYAJI and T. KOKUBO, *J. Am. Ceram. Soc.* **78**(9) (1995) 2405.
10. W. CAO and L. L. HENCH, *Ceram. Int.* **22** (1996) 493.
11. H. M. KIM, F. MIYAJI, T. KOKUBO, C. OHTSUKI and T. NAKAMURA, *J. Am. Cer. Soc.* **78**(9) (1995) 2405.
12. E. VERNÉ, R. DEFILIPPI, C. VITALE BROVARONE, G. KARL and J. VOGEL, *Materials for Medical Engineering* **2** (2000) p. 140.
13. E. VERNÉ, C. VITALE BROVARONE and D. MILANESE, *J. Biom. Mat. Res. (Appl. Biom.)* **53** (2000) 408.
14. E. VERNÉ, C. VITALE BROVARONE, C. MOISESCU, E. GHISOLFI and E. MARMO, *Acta Mater.* **48** (2000) 4667.
15. E. VERNÉ, E. BONA, A. BELLOSI, C. VITALE BROVARONE and P. APPENDINO, *J. Mat. Sci.* **36** (2001) 2801.
16. C. VITALE BROVARONE, E. VERNÉ, A. KRAJEWSKI and A. RAVAGLIOLI, *J. Eur. Cer. Soc.* **21** (2001) 2855.
17. E. VERNÉ, M. BOSETTI, C. VITALE BROVARONE, C. MOISESCU, F. LUPO, S. SPRIANO and M. CANNAS, *Biomaterials* **23** (2002) 3395.
18. C. KLEIN, K. DE GROOT, C. WEIQUN, L. YUBAO and Z. XINGDONG, *ibid.* **15** (1994) 31.
19. M. FABBRI, G. C. CELOTTI and A. RAVAGLIOLI, *ibid.* **16** (1995) 225.
20. A. TAMPIERI, G. CELOTTI, S. SPRIO, A. DELCOGLAINO and S. FRANZESE, *ibid.* **22** (2001) 1365.
21. N. L. PORTER, R. M. PILLIAR and M. D. GRYNPAS, *J. Biomed. Mater. Res.* **56** (2001) 504.
22. H. YUNA, J. DE BRUJIN, X. ZHANG, C. VAN BLITTERSWIJK and K. DE GROOT, *ibid. (Appl. Biomater.)* **58** (2001) 270.
23. O. LYCKFELDT and J. M. L. FERREIRA, *J. Eur. Cer. Soc.* **18** (1998) 131.
24. A. F. LEMOS and J. M. F. FERREIRA, *Mat. Sci. End. C* **11** (2000) 35.
25. M. H. PRADO DA SILVA, A. F. LEMOS, I. R. GIBSON, J. M. F. FERREIRA and J. D. SANTOS, *J. Non-Cryst. Solids* **304** (2002) 286.
26. H. RAMAY and M. ZHANG, *Biomaterials* **24** (2003) 3293.
27. O. PEITL, E. ZANOTTO and L. HENCH, *J. Non-Cryst. Solids* **292** (2001) 115.
28. N. SARIS, E. MERVAALA, H. KARPPANEN, J. KHAWAJA and A. LEWENSTAM, *Clin. Chimica Acta* **294** (2000) 1.
29. J. VORMANN, *Mol. Aspects Med.* **24** (2003) 27.
30. E. JALLOTS, *Appl. Surf. Sci.* **211** (2003) 89.
31. H. M. KIM, F. MIYAJI, T. KOKUBO, C. OHTSUKI and T. NAKAMURA, *J. Am. Cer. Soc.* **78**(9) (1995) 2405.

Received 9 December 2002
and accepted 12 September 2003